

Experimental Evaluation of the Mobile Radio Channel Capacity in the 2.48 GHz Band

Uwe R. Villanueva and Gláucio L. Siqueira

*Pontifical Catholic University of Rio de Janeiro CETUC/PUC-Rio, Rio de Janeiro, Brazil
uweojas@gmail.com and glaucio.siqueira@puc-rio.br*

Leni J. Matos and Pedro V. G. Castellanos

Fluminense Federal University, Niterói, Rio de Janeiro, Brazil, lenijm@id.uff.br and pcastellanos@id.uff.br

Leonardo H. Gonsioroski

*Maranhão State University, São Luís, Maranhão, Brazil
gonsioroski@uema.com*

Abstract— This paper deals with the effect of the Single-Input Multiple-Output spatial diversity on the OFDM mobile radio signal propagating in an urban channel. From measurements performed in Rio de Janeiro city, Brazil, by using two receiving antennas at diversity, the calculated capacity presented an improvement when compared to the individual one.

Index Terms— delay spread, OFDM, SIMO, spatial diversity, urban channel.

I. INTRODUCTION

Over the last years, the OFDM (Orthogonal Frequency Division Multiplexing) technique has received special attention to the mobile radio communication in the cellular systems [1-3]. Since the available bandwidth is divided into narrower bands, each one experimenting flat fading, this technique presents robustness against time-varying frequency-selective fading. Therefore, such technique offers advantages considering its ability in dealing with high-data-rate transmissions over dispersive channels with low equalization complexity [3]. It is also an efficient solution to operate in Non-Line-Of-Sight (NLOS) conditions, normally subject to multipath fading, because it uses cyclic prefix (CP) in order to avoid intersymbol interference. However, the mobility demanded by the users degrades the received signal, worsening it due to the increasing speed which leads a Doppler shift that desynchronizes the OFDM subcarriers, consequently, causing intercarrier interference [4].

There have been some solutions to improve final user's delivered signal. Among them is the spatial diversity which is most referred in several studies and it has been used in the reception of the OFDM signal. Ali et al. deals with simulations of blind estimation techniques that exploit the receive antenna diversity [5]; Yagishita et al. [6] studies the effects of diversity in the receiving antenna using Faster-than-Nyquist (FTN) signaling in a multipath fading channel; Kim et al. [7] analyzes the macro-diversity in LTE-Advanced. However, most of results presented in those studies were obtained from simulations. In this context, this paper provides experimental results for the capacity obtained in a 2.48 GHz band using the spatial diversity in a SIMO (Single-Input Multiple-Output) system. Two branches were used in the reception of a 40 MHz-OFDM signal in the 2.48 MHz band. In order to accomplish it, an urban channel was sounded and the signals from both branches of diversity were

simultaneously and independently obtained and processed off-line. The capacity per band (in bps/Hz) of each branch was calculated and compared to the SIMO capacity.

For such purpose, this paper consists of five additional sections. Section II describes the specifications of the system and the environment sounded in the measurements, in addition to the OFDM signal transmitted to the channel; Section III provides a brief summary of the channel function and the capacity calculation for SISO (Single-Input Single-Output) and SIMO systems; Section IV presents the results, and Section V provides the conclusion.

II. MEASUREMENT ENVIRONMENT AND SYSTEM SPECIFICATIONS

Fig. 1 presents the sounded area where measurements were carried out which covers Gávea, Leblon and Lagoa surroundings in Rio de Janeiro. The transmitting station was installed at Kennedy building located at PUC-Rio University, [8]. The sounded area was characterized as an urban area and the arrows show the sense of the movement during the sounding of the channel.

The transmission setup includes a vector signal generator, a power amplifier and a vertically polarized sector antenna fixed on the geographical coordinates $22.978976^{\circ}\text{S}/ 3.232598^{\circ}\text{W}$. The antenna was placed on the top of a 49 m high building. The receiving equipment was installed inside a moving vehicle, at an average speed of 65 km/h. Two omnidirectional antennas and two branches of reception and a Garmin GPS (Global Positioning System) were mounted on its top. The reception setup for the wideband channel sounder was employed according to Gonsioroski [9] using the multicarrier technique, however, two branches of diversity were here used. Table I provides the main specifications of the transmission (TX) and the reception (RX) system.



Fig. 1. Aerial view of the sounded region. (Source: Google earth).

TABLE I. TRANSMITTER AND RECEIVER SPECIFICATIONS

	Device	Specifications
Tx	Vector Signal Generator MG3700A	250 kHz to 6 GHz
	Power Amplifier Milmega, model AS0204-7B 2-4 GHz 7W	G = 47 dB
	Antenna Pctel SP232715XP-90	G = 16 dBi
	Broadband Low Noise Amplifier ABL0800-12-3315	G = 33 dB
Rx	Vector Signal Analyzer MS 2692A	50 Hz to 26,5 GHz
	Antenna Superbat 700 - 2600 MHz 4G LTE omnidirecional	G = 5 dBi
	GPS Garmin GPSmap62	-

Fig. 2 illustrates the RX setup that operates with two identical antennas separated by 0.50 m distance (d), placed on the roof top of a van. Inside the van, the reception system for each antenna was separated and each one consisted of one low noise amplifier (LNA), a vector signal analyzer and a dedicated computer. The analyzer collected the samples in quadrature, in a 100 Msamples per second rate. The spacing used between the antennas certifies the decorrelation between the received signals (s and s') from both branches of diversity. The verification was possible by calculating the correlation between them through the Pearson correlation coefficient [10], defined as:

$$C = \frac{\sum_{i=1}^n (s_i - \bar{s}) \cdot (s'_i - \bar{s}')}{\sqrt{\sum_{i=1}^n (s_i - \bar{s})^2} \cdot \sqrt{\sum_{i=1}^n (s'_i - \bar{s}')^2}} \quad (1)$$

with s_i and s'_i representing the samples of the signals in each antenna and s and s' representing the arithmetic means of s and s' , respectively. The calculated value was $C = 0,0061$, i.e., the correlation between the signals received from the antennas is equal to 0,61% indicating a negligible correlation, which confirms that $0,50\text{ m}$ guarantees good decorrelation.

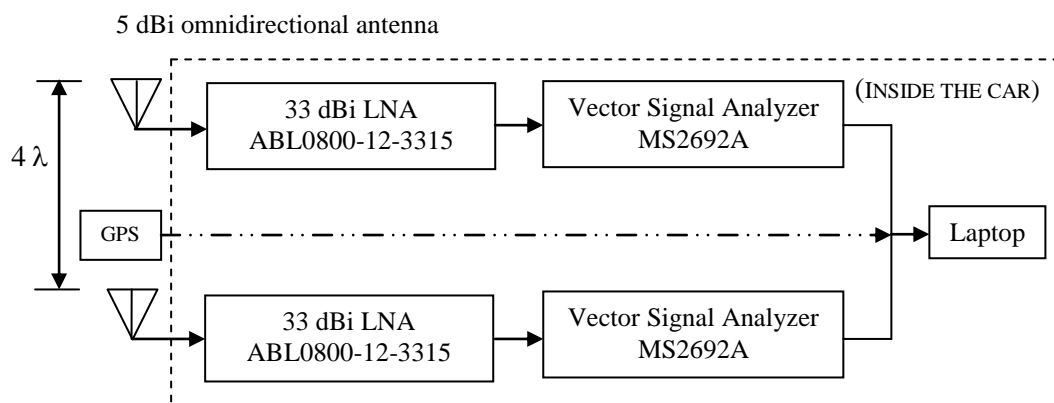


Fig.2. Diversity reception system.

III. TRANSMITTED SIGNALS AND PROCESSING

A. OFDM Transmitted Signal

Table II shows the main characteristics of the OFDM signal that was generated in MATLAB[®] software. The spectral efficiency of this signal is assured by the orthogonality of the subcarriers, which are linearly independent. Like occurred in Gonsioroski [9], the OFDM signal was modulated

by a pseudo-noise (PN) sequence of 2047-bits length. The number of OFDM samples ($N_{\text{FFT}} = 2048$) was increased by $1/16 \times N_{\text{FFT}}$, which corresponds to the cyclic prefix interval inserted between the OFDM symbols to accommodate the time dispersion of the signal that arrives at the receiver. Via network cable, the modulated signal was conducted to the vector signal generator, which sent the signal on the 2.48 GHz carrier to the power amplifier, followed by the antenna and for radiating and sounding the channel. Such sequence helped to identify the OFDM symbols in the off-line processing because of its correlation property [11].

TABLE II. MAIN PARAMETERS OF THE OFDM TEST SIGNALS

Parameter	Value	Unit
Bandwidth	40	MHz
Size of the FFT	2048	Samples
Sampling Factor	2	-
Sampling Rate	100×10^6	Samples/second
Number of Carriers	1600	Carriers
Cyclic Prefix	1/16	Samples

B. Channel response

In order to determine the capacity of the experimental channel, the channel gain must be calculated in each diversity branch. For that purpose, the data acquired from the measurements were saved in I (*In-phase*) and Q (*Quadrature*) components, therefore, the samples are complex values. From them, the mean power of each OFDM symbol (S) was calculated.

The mobility of the receiver leads to a time variant channel and its impulsive response is shown in the time/delay domain, i.e., $h(t, \tau)$, which means the response in a t instant of an impulse sent τ seconds before [12]. For that reason, the mobility results, in different responses, during the same channel monitoring time. As far as the WSSUS (Wide Sense Stationary Uncorrelated Scattering) condition is concerned, the channel can be represented by a unique $h(t, \tau)$ random function.

In the sequel, the received data were convolved with a filter matched to the transmitted signal in order to provide the channel impulse response as can be demonstrated as follows.

Supposing that $s(t)$ corresponds to the signal transmitted through a channel and that $s'(t, \tau)$ refers to the signal that arrives at the reception as a sum of N multipath of the transmitted signal, whose amplitudes are represented as a_i , delays as τ_i e phase as φ_i , i.e.:

$$s'(t, \tau) = \sum_{i=1}^N a_i e^{j\varphi_i} s(t - \tau_i, \tau), \tag{2}$$

disregarding the modulation, and taking $C_i = a_i e^{j\varphi_i}$ in (2), the received signal is:

$$s'(t, \tau) = \sum_{i=1}^N C_i s(t - \tau_i, \tau) \tag{3}$$

The matched filter is defined as:

$$h_{FC}(t, \varphi) = s(-t, \tau) \tag{4}$$

Therefore, the signal after the matched filter is:

$$y(t, \tau) = s'(t, \tau) * h_{FC}(t, \tau) \tag{5}$$

Convolving (3) and (4) and substituting in (5):

$$y(t, \tau) = \sum_{i=1}^N C_i \int_{-\infty}^{\infty} s(\xi - \tau_i, \tau) s(-t + \xi, \tau) d\xi \tag{6}$$

$$y(t, \tau) = \sum_{i=1}^N C_i R_s(t - \tau_i, \tau) \tag{7}$$

If $s(t, \tau) = \delta(t, \tau)$ is an impulsive signal at the input of the channel, the impulsive response is the output of the channel, i.e.:

$$s'(t, \tau) = h(t, \tau) \tag{8}$$

Comparing this identity to (3), the impulsive response is:

$$h(t, \tau) = \sum_{i=1}^N C_i s(t - \tau_i, \tau) \tag{9}$$

As $s(t, \tau) = \delta(t, \tau)$, thus $s(t - \tau_i, \tau) = \delta(t - \tau_i, \tau)$, which is substituted in (9), obtaining:

$$h(t, \tau) = \sum_{i=1}^N C_i \delta(t - \tau_i, \tau) \tag{10}$$

Substituting $s(t, \tau) = \delta(t, \tau)$ in (5), the autocorrelation $R_s(t - \tau_i, \tau)$ can be simplified to $\delta(t - \tau_i, \tau)$ and we conclude that the output of the matched filter in (5) corresponds to the transfer function of the channel in (10) when an impulsive input is used. In short, with a transmitted signal as similar as an impulse it will be possible achieve the transfer function of a channel, if the received signal passes through a matched filter. Therefore, the absolute value of the power delay profiles (PDPs) for the sounded channel [12] can be calculated as:

$$P_h(t, \tau) = |h(t, \tau)|^2 \tag{11}$$

and $P_h(t, \tau)$ represents the complex power of all multipath that arrive at the receiver antenna in each time instant. Fig. 3 exemplifies two PDPs obtained at the same time in the RX antennas, showing different multipath receptions from different branches of diversity. PDPs and GPS positions were saved in files. Through the profiles obtained, it was possible to observe and analyze the dispersiveness of the channel. The variation of RMS (Root Mean Square) delay spread [12] calculation is demonstrated in Table III for each diversity link named L1 (related to antenna 1) and L2 (related to antenna 2). Such values show that the sounded channel was not WSSUS since the dispersion

parameters had a large variation and just one PDP was not able to represent the channel. In this case, the time-variant channel does not allow us to consider stationarity, which can only be applied in small intervals of the measured path [12]. Consequently, the channel gain is a variable.

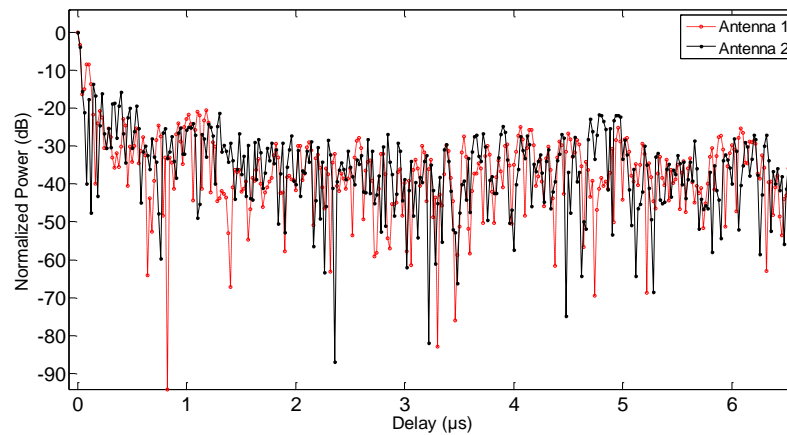


Fig. 3. PDPs of two diversity branches.

According to the results, the time dispersion along all paths varies around 2 microseconds, from hundreds of nanoseconds until some microseconds, which leads us to conclude that the channel behaves as an urban one at most of the time, and varies between less dense to more dense [8], [12].

TABLE III. TEMPORAL DISPERSION PARAMETERS.

Antenna	Link	RMS Delay Spread (μs)
1	L1	0.172 - 4.438
2	L2	0.223 - 4.253

The mean noise power (P_N) in each OFDM symbol was also calculated as [13]:

$$P_N = 10 \log_{10} \left[B_s \cdot \frac{\sum_{i=1}^n 10^{P_i/n}}{NBW} \right] \quad (12)$$

in which:

$$NBW = 1.065 \times RBW \quad (13)$$

and RBW is the band of the resolution filter used in the spectrum analyzer, NBW is the equivalent band of noise spectrum, B_s is the band of the transmitted symbol (40 MHz), n is the number of the noise samples inside the band of 40 MHz and P_i is the power of each noise sample. Such samples were obtained along the route without turning on the transmitter, only acquiring noise samples and saving them for post processing. The measured noise of the channel was -141 dBm/Hz. In the 2.48 GHz band the ambient noise floor was limited by the noise floor [14] of the measurement system and it was not possible to acquire measurements in the 1250-2700 m range. By using the `dfitool` function of Matlab®, the amplitude samples of the noise presented a better adjustment to the Gaussian statistics, therefore, allowing us to use the most largely equations found in literature for calculating channel capacity as described next.

C. Capacity in SISO and SIMO systems

If compared to a SISO, either SIMO or MISO (Multiple-Input Single-Output) systems can provide significant improvement in communication quality (bit error rate - BER) as well as in capacity, by using multiple antennas to provide space diversity. The expressions needed to calculate capacity in bps will be provided in the following paragraph.

For an out of memory system, the maximum capacity of a wideband SISO system in a Gaussian channel is written by [15]:

$$C_{SISO} = B \cdot \log_2(1 + \rho |h|) \quad (14)$$

in which ρ is the mean signal-to-noise ratio ($SNR = S/P_N$) at the receiving antenna and $h(t, \tau)$ is the complex channel gain.

The same process occurs in memoryless wideband SIMO system, in which each reception channel is independent from the other, if ρ is a constant mean in the environment of a Gaussian noise, the maximum channel capacity, in bps, is calculated from:

$$C_{SIMO} = B \cdot \log_2 \left(1 + \rho \sum_{i=1}^N |h_i|^2 \right) \quad (15)$$

in which h_i is the channel gain related to each branch of diversity, therefore, $|h_i(t, \tau)|^2$ means the absolute value of the power delay profile and n is the number of receiver antennas.

In a random time variant channel, the maximum capacity, due to the diversity in a SIMO receiver, is calculated from [14]:

$$C_{SIMO} = B \cdot \log_2 \{ \det [1 + \rho H H^H] \} \quad (16)$$

with H meaning the $N \times 1$ channel gain, H^H is the transposed matrix of H , and N is the number of receiver antennas. In this test two diversity branches were used, therefore:

$$C_{SIMO} = B \cdot \log_2 \{ 1 + \rho |H_{11}|^2 + \rho |H_{22}|^2 \} \quad (17)$$

in which H_{11} and H_{22} represent the channel gains on the diversity branches TX-RX1 and TX-RX2, respectively.

IV. RESULTS

Fig. 4 depicts the OFDM power levels signal received along the whole route. Those values were obtained in the marked distances associated to different time instants. In most cases, they decreased up to 1250 meters. LOS and NLOS links appear throughout that distance. From approximately 1250 to 2700 m, the received power level remained below the spectrum analyzer threshold. When distance reached 2700 m length, peaks and valleys of power were detected. In the final distances high values were observed and they occurred due to the contribution of water reflections and the LOS link since the receiver was opposite of the transmitter, across the lagoon (Fig. 1). For that reason, only up to 1

km distances were considered were considered for diversity gain calculation.

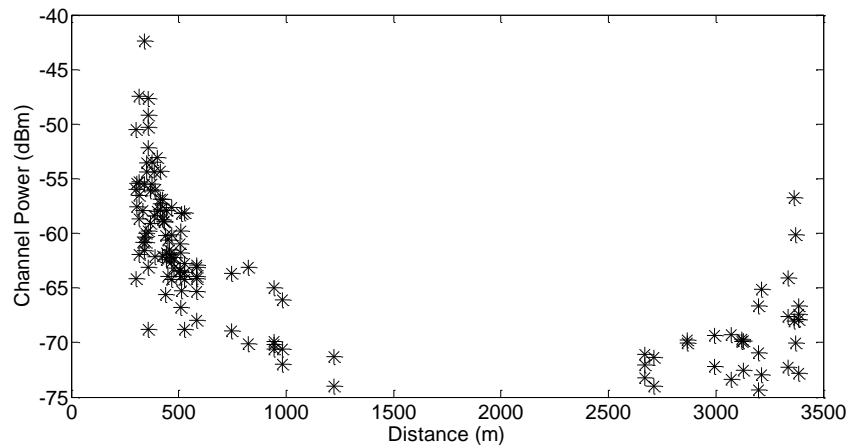


Fig. 4. Power level of the received signal along the whole route.

Neither ρ (\equiv SNR) nor the channel gain, $h(t, \tau)$, remained constant in the entire sounded route in Fig. 1. Consequently, equations (14) and (17) were calculated for each power delay profile obtained related to received OFDM symbol. Different capacities per band are depicted in Fig. 5 for both diversity branches, confirming that the capacity proportionally increased with the SNR.

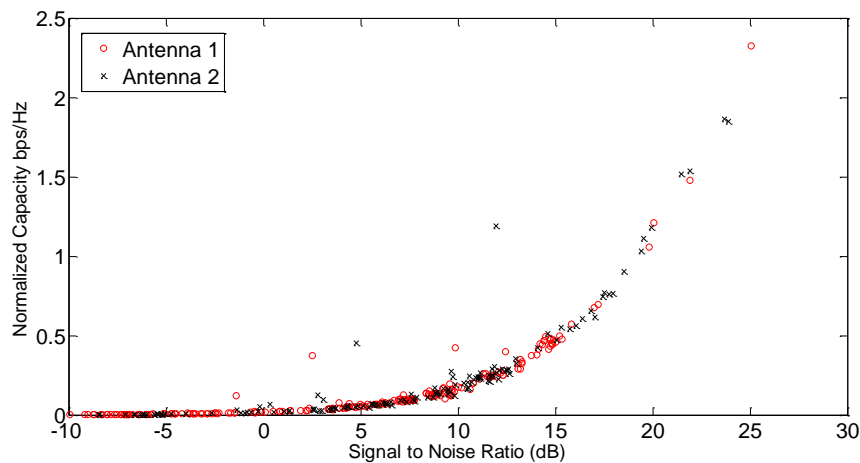


Fig. 5 - Capacity/band versus SNR for both diversity branches.

Fig. 6 shows capacities decreasing while transmitter distance increases. The curve shows the SIMO values capacity adjustment, which resulted in a capacity gain as the application of spatial diversity was used. However, the capacity gain is better performed in smaller distances since the mean signal power decreases with distance and strongly affects the capacity calculus, whereas the mean noise signal practically remains the same.

The results are compacted in Table IV in which improvement on capacity can be observed as well as those found in literature related to simulations [16].

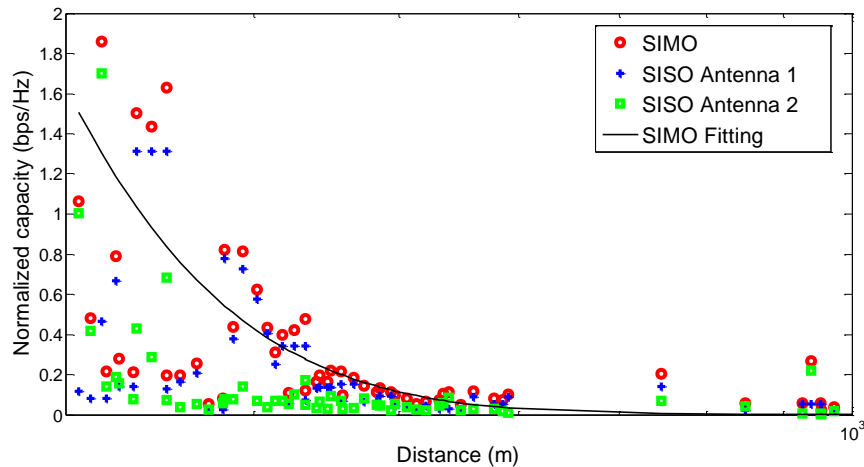


Fig. 6. Experimental capacity/band.

TABLE IV. EXPERIMENTAL CAPACITY

Capacity/band	bps/Hz	Transmission rate (Mbps)
SISO - Branch 1	0.003 to 1.3	0.12 to 52
SISO - Branch 2	0.007 to 1.7	0.28 to 68
SIMO - Branches 1 and 2	0.100 to 1.86	4.00 to 74.4

V. CONCLUSIONS

It is essential to study the channel behavior in urban areas for implementing LTE technology and reaching a good system planning, searching for the transmission rate possible in this kind of channel. Such rate is low in this environment typically urban, in general, and the diversity technique is one of the possible solutions to increase it.

In order to evaluate the experimental results of the 1 x 2 SIMO system, measurements on the 2.48 GHz band were carried out in an outdoor channel. OFDM symbols of 40 MHz were transmitted and the channel response was calculated. With two omnidirectional antennas in the reception side, I and Q samples of the wideband signal were acquired independently at both diversity branches. By matched filtering of the complex signal measured, the power delay profiles were determined. The results for the RMS delay spread are typical of a urban environment with values from not overcoming 4 μ s. Such results permit maximum transmission rates that vary from hundreds of kbps to some Mbps [17]. It is worth to say that these are raw rates with no equalization or codification applied.

The noise power and the signal power of the OFDM were calculated for obtaining the signal-to-noise ratio. Finally, the channel capacity was calculated for each reception branch and also combined for providing the total capacity of the SIMO system. On the branch 1 of diversity, the rate varied from 0.12 to 52 Mbps while its varied from 0.28 to 68 Mbps on the branch 2. Accordingly, the transmission rate using the 1 x 2 SIMO system without other resources as equalization or codification has presented a better transmission rate, yielding rates varying from 4 to 74.40 Mbps, depending on the distance between the transmitter and the receiver. It shows a mean improvement over the individual

ones of 1.24 Mbps for the antenna 1 and 9.26 Mbps for the antenna 2. Thus, the spatial diversity improved the mean transmission rate. These results are not so good as those obtained in indoor channels [18], in which there is more contribution of multipath, in general, and they have used MIMO instead of SIMO. However, they are inside the range simulated by Cueto et al. [16] in which mean values of throughput ranged from 0.025 to 2.85 bps/Hz for a 40 MHz OFDM transmitted in modulations increasingly robust, varying from QPSK with 1/8 code rate to 64 QAM with 3/4 code rate.

In future works, 1 x 2 SIMO system will be experimentally tested, including other urban channels, in order to verify the improvement in the spectral efficiency on this kind of channel. Moreover, 1 x 3 SIMO will be tested and comparisons will be made with 2 x 2 MIMO.

ACKNOWLEDGEMENT

Author thanks CAPES for the scholarship provided.

REFERENCES

- [1] J. P. Niu, D. Lee, X. Ren, G. Li, and T. Su, "Scheduling Exploiting Frequency and Multi-User Diversity in LTE Downlink Systems", *IEEE Trans. on Wireless Communications*, vol. 12(4), pp. 1843-1849, April 2013.
- [2] J. G. Andrews, A. Ghosh, and R. Muhamed, *Fundamentals of WiMAX: Understanding Broadband Wireless Networking*, Prentice Hall, 2007.
- [3] Y. G. Li and G. L. Stuber, *Orthogonal Frequency Division Multiplexing for Wireless Communications*, Springer, 2006.
- [4] Y. G. Li and L. J. Cimini, "Bounds on the interchannel interference of OFDM in time-varying impairments", *IEEE Trans. on Communications*, vol. 49, no. 3, pp. 401-404, March 2001.
- [5] H. Ali, A. Doucet, and Y. Hua, "Blind SOS subspace channel estimation and equalization techniques exploiting spatial diversity in OFDM systems", *Digital Signal Processing*, Springer, vol. 14, no. 2, pp. 171-202, March 2004.
- [6] K. Yagishita, Y. Kakishima, and M. Sawahashi, "Effects of antenna receiver diversity with Faster-than-Nyquist signaling using OFDM/OQAM in multipath fading channel", *International Symposium on Wireless Personal Multimedia Communications (WPMC)*, 2014, pp. 351-355, Sep. 2014.
- [7] G. B. Kim, J. Lee, Jac, and S. J. Hong, "Analysis of Macro-Diversity in LTE-Advanced", *KSII Trans. on Internet and Information Systems*, vol.5(9), pp.1596-1612, Sep. 2011
- [8] U. R. Villanueva, G. L. Siqueira, L. J. Matos, L. H. Gonsioroski and P. V. G. Castellanos, "Propagation Channel Characterization in the 2.48 GHz Frequency Band in an Urban Area", in IMOC'15, PE, Brazil, 2015, pp. 1-5.
- [9] L. H. Gonsioroski, L. da Silva Mello, C. R. Ron, and L. J. Matos. (2015, vol. 14). Characterization of a Mobile Urban Radio Channel with an Improved Multicarrier Sounding Technique, *Journal of Microwaves, Optoelectronics and Electromagnetic Applications* [Online], SI-158-SI-167. Available: <http://www.jmoe.org/index.php/jmoe/article/view/517>.
- [10] J. Benesty et al., *Noise Reduction in Speech Processing*, Springer-Verlag Berlin Heidelberg, 2009.
- [11] M. Goresky and A. Klapper, "Pseudonoise Sequences Based on Algebraic Feedback Shift Registers", *IEEE Trans. on Information Theory*, vol. 52, no. 4, April 2006, pp. 1649-1662.
- [12] J. D. Parsons, *The Mobile Radio Propagation Channel*, John Wiley & Sons, 2nd. Ed., 2000.
- [13] C. Rauscher, *Fundamental of Spectrum Analysis*, Rohde & Schwarz, Germany, 2001.
- [14] R. Leck, Results of Ambient RF Environment and Noise Floor Measurements Taken in the U.S. in 2004 and 2005, *Commission for Basic Systems Steering Group on Radio Frequency Coordination*, 1-18 March 2016.
- [15] D. Tse and P. Viswanath, *Fundamentals of Wireless Communication*, USA, Cambridge University Press, 2005.
- [16] D. Y. N. Cueto, L. A. R. Silva Mello, and C. V. R. Ron, "Comparison of Coverage and Capacity of LTE-Advanced Networks at 700 MHz and 2.6 GHz", IMOC 2013, RJ, Brazil, 2013, pp. 1-5.
- [17] T. S. Rappaport, *Wireless Communications – Principles and Practice*, Prentice Hall, 1996.
- [18] B. Mnasri, M. Nedit, N. Kandil, L. Talbi, and I. B. Mabrouk, "Experimental Characterization of wireless MIMO Channel at 5.8 GHz in Underground Gold Mine", *Progress In Electromagnetics Research C*, vol. 36, pp. 169-180, 2013.